参赛学生姓名: Linda Su Zhao
中学: Tsinghua International School Daoxiang Lake
省份: Beijing Beijing
O -7/N
国家/地区: China
指导老师姓名: Zhen-Chuan Fan, Han Wang
THE TENT PLANT CHANGE THE TENT WANTED
指导老师单位: Zhejiang University, Tsinghua
International School Daoxiang Lake
论文题目: <u>Multiscale study on the effect of Tubby-like</u>
protein 2 on cilia-driven motility behavior of
Chlamydomonas reinhardtii
Co. Liv
02.14
V ·

Multiscale study on the effect of Tubby-like protein 2 on ciliadriven motility behavior of *Chlamydomonas reinhardtii*

Linda Su Zhao

1. Abstract

Cilia are motile and sensory organelles widely present in eukaryotic cells, and their dysfunction is closely associated with various human ciliopathies. Tubby-like proteins (TLPs) play critical roles in ciliary assembly and signal transduction; however, whether and how TLP2 regulates ciliary motility remains insufficiently studied. To elucidate the role of TLP2 in cilia-driven motility, this study employed *Chlamydomonas reinhardtii* as a model organism and integrated a suite of techniques including population-based phototaxis assays, single-cell motility tracking, cell micromanipulation, and AI-assisted image analysis to comprehensively compare the motility characteristics of wild-type (CC-5325) and TLP2 knockout mutant (tlp2) across populational, cellular, and ciliary scales. The results demonstrated that compared with CC-5325, tlp2 completely lost phototaxis, exhibited significantly reduced swimming speed, and showed a shift from linear trajectories in CC-5325 to more tortuous-like ones. By developing an AI-assisted tool for the image analysis, the beating behavior of the two cilia of a cell were further analyzed: in CC-5325, the two cilia of a cell beat synchronously, whereas in tlp2, the two cilia displayed an asynchronized beating with the beating periods of the two cilia differed significantly (0.029 s vs. 0.038 s, respectively). This can directly explain the motility differences of the two strains observed at the cellular and populational scales. The findings of this study demonstrate the important roles of TLP2 in the regulation of cilia-driven motility, which can provide insight for developing new strategies in combating cilia-related diseases, especially oligoasthenoteratozoospermia.

Keywords: Cilium/flagellum, motility, Tubby-like protein, C. reinhardtii

Table of Contents

1.	Abstract2		
2.	Introduction4		
	2.1	Research background	
	2.2	The aim and content of this study6	
	2.3	Significance of this study	
3.	Materials and Methods		
	3.1	Chlamydomonas strains	
	3.2	Population phototaxis assay	
	3.3	Microscopic observations of cells	
	3.4	Micromanipulation of cells9	
	3.5	Image analysis9	
4.	Results		
	4.1	C. reinhardtii cells lost phototactic behavior in the absence of TLP210	
	4.2	tlp2 showed different characteristic swimming motility than WT cells 11	
	4.3	The swimming motility differences between two strains arise from different	
	beatir	ng behavior of cilia14	
	4.4	Statistical analysis of immobilized cells through micromanipulation	
	revea	led the impaired synchronization of ciliary beating in <i>tlp2</i> cells20	
5.	Discu	ssions24	
6.	Conclusion		
7.	References		
8.	Legends of supplementary movies		
9.	Acknowledgement		

2. Introduction

2.1 Research background

Cilia/Flagella are hair-like surface appendages existing in many types of eukaryotic cells, ranging from unicellular organisms like algae to mammalian cells such as lung epithelium and sperm cells^{1,2}. A single cilium is composed of a basal body, an axoneme and cilia membrane (Figure 1)¹. The axoneme is a tube-shaped structure that has a typical 9+2 microtubule structural arrangement with 9 outer microtubule doublets surrounding a central pair of microtubules. Nexins link neighboring outer microtubule doublets while each outer doublet also has protein complexes called "radial spokes" extended toward the central pair. There are two arms, outer dynein arm and inner dynein arm, associated with each outer doublet, which serve as molecular motors and drive the beating of cilia². Besides motile cilia, there are also non-motile cilia (known as primary cilia), which typically has a 9+0 arrangement².

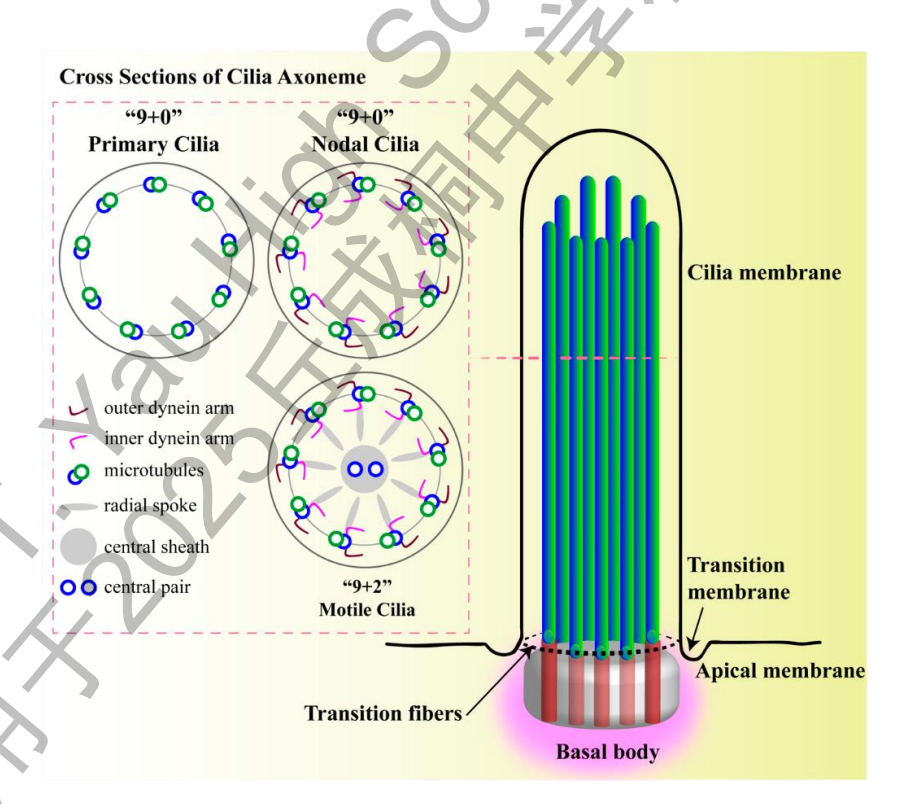


Figure 1. Sketch of a cilium structure. Figure adapted from reference¹.

Cilia act as either a motility unit or sensory organelles, and thus play important

roles in cell motility, growth and adaptation to local environment. For instance, *Chlamydomonas reinhardtii* (*C. reinhardtii*) use cilia to perform phototaxis, by which cells can find appropriate illumination conditions for cell photosynthesis^{3,4}. In mammals like humans, dysfunction of cilia often lead to ciliopathies⁵. For instance, dysfunctions of motile cilia will result in male infertility and primary ciliary dyskinesia (PCD)⁶ while defects in primary cilia are closely related to diseases including polycystic kidney disease (PKD), Bardet-Biedl syndrome (BBS), retinitis pigmentosa (RP) and orofaciodigital syndrome (OFD)⁵. Many of them such as BBS, RP and OFD are rare genetic diseases. Thus, it is necessary to understand the mechanisms and regulations of ciliary assembly and functions, to find effective ways to battle these diseases.

Tubby-like proteins (TLPs for plants and algae, and TULPs for mammals) are widely found in eukaryotic cells and play important roles in cell development. In mammalian cells, there are five types of TULPs (TUB, TULP1, TULP2, TULP3, TULP4)⁷. Among them, TUB, TULP1 and TULP3 have been studied extensively. TUB is the first discovered protein of TULP family in mice, and it has been shown to be related to obesity, retinal degeneration, and hearing loss of mice^{8,9}. TULP1 is found to be closely related to eye diseases¹⁰ while TULP3 is vital in embryonic neural development¹¹. More generally, TULP3 (TLP3 in C. reinhardtii) also act as a general adapter for intraflagellar transport (IFT) of membrane-associated proteins such as G protein-coupled receptors 12, which are important for ciliary functions. In contrast to the widely recognized functions of TUB, TULP1 and TULP3, TULP2 and TULP4 are relatively less understood. Recently, however, studies show that TULP2 plays an important role in affecting spermatogenesis¹³. Tulp2 was found to be specifically expressed in the testis of mice, and lacking TULP2 would lead to the phenotype of oligoasthenoteratozoospermia: the decreased sperm count and tail deformity of spermatozoa, implicating its potential role in male fertility¹³. In addition, at the ciliary tip of Tetrahymena thermophila, TLP2 is found to help maintain the integrity of the axoneme of cilia by wrapping laterally around and linking the central two

microtubules¹⁴. Together, these results suggest that TLP2/TULP2 is related to the assembly and/or functions of cilia, but the mechanisms are largely unknown. Particularly, how the cilia beating pattern would be altered due to TLP2/TULP2 disruption and its associated phenotypical motility behavior remain to be discovered.

Chlamydomonas reinhardtii, a green alga, has two motile flagella/cilia. Here, the term cilium and the flagellum are interchangeable, as their structures are virtually identical². C. reinhardtii cells can swim in aqueous environment through cilia beating in a form of breaststroke. They also contain an organelle called eyespot, by which cells can sense light signals and then respond by altering their cilia beating patterns accordingly (e.g., phototaxis)^{3,4}. Compared with mammalian cells, C. reinhardtii is a simpler organism, and has a vast of genetic tools for engineering. All these merits make it an ideal model organism for cilia/flagella-related studies. For instance, recent studies on BBSomes¹⁵⁻¹⁷ in C. reinhardtii cells have greatly advanced our understandings on the mechanisms of IFT activities of cilia, which are vital for enabling cells to sense and transduce extracellular stimuli inside the cell.

2.2 The aim and content of this study

In this study, we chose *C. reinhardtii* as the model system, and employed microbial microscopic tracking techniques, which enable us to monitor the microbial behavior in a real-time and in situ manner. By studying the motility behavior of wild-type (WT) *C. reinhardtii* strain and a TLP2-null mutant, we aim to understand mechanistically how the motility behavior of *C. reinhardtii* will be affected by TLP2, thus, to reveal the role of TLP2 in the regulation of cilia-driven motility of cells.

Toward the goal, we have studied the motility behavior of *C. reinhardtii* cells from three different scales: Firstly, at the populational scale (i.e., macroscopic level), by employing petri dish-based phototaxis assays, we analyzed the differences in phototactic behavior between WT (CC-5325) and TLP2 knockout mutant (*tlp2*) to evaluate the role of TLP2 in the regulation of cell light-responses. Secondly, at the cellular scale (i.e., mesoscopic level), through high temporal-resolution microscopic tracking techniques, we quantified and compared the cellular movement ratio,

locomotion velocity, and movement trajectories of both algal strains to elucidate the role of TLP2 in the overall regulation of motility. Thirdly, at the ciliary scale (i.e., microscopic level), we performed micromanipulation experiments and observed the beating patterns of individual cilium and combined with high-speed microscopic imaging to analyze whether TLP2 deficiency causes abnormal ciliary beating. In addition, to analyze the data more efficiently, we developed an AI-assisted method to perform image analysis in a high-throughput way.

2.3 Significance of this study

The results of this study quantitatively described the motility behavior of *C. reinhardtii* from three different scales. Such multiscale description clearly and comprehensively illustrated different motility behavior of TLP2 mutant compared with WT cells. These results will help to further understand the roles of TLP2 in the regulation of cilia-driven motility and thus provide insight for developing new strategies in combating flagella/cilia-related diseases. Moreover, the developed high-throughput AI-assisted image processing method provides a useful tool for data processing of microscopic images and can be readily extended to other related scenarios.

3. Materials and Methods

3.1 Chlamydomonas strains

The WT *C. reinhardtii* strain CC-5325 and *tlp2* mutant were obtained from Prof. Zhen-Chuan Fan's lab. Unless otherwise specified, axenic cultures were maintained in Tris-Acetate-Phosphate (TAP) medium (pH 7.0 ± 0.2) under controlled environmental conditions: 23 ± 1 °C with continuous illumination at 100 µmol photons/m²/s provided by cool-white fluorescent lamps.

3.2 Population phototaxis assay

C. reinhardtii was cultured until the optical density at 680 nm (OD₆₈₀) reached \geq 0.7. For each assay, 10 mL of algal suspension was equally aliquoted into two separate 15 mL centrifuge tubes and centrifuged at 3,000 rpm (×g relative centrifugal force) for 5 min. Following complete cell sedimentation, approximately 3 mL of supernatant was

removed by pipetting, leaving a concentrated cell pellet. The pellet was resuspended and transferred using a 20 μ L precision pipette to the central region of a 30 mm glass-bottom dish, ensuring complete coverage of the observation area. Uniform cell dispersion was achieved through gentle repetitive pipetting. Phototactic behavior was induced using a unilateral white LED illumination system (light intensity precisely controlled at $\sim 6.32 \times 10^{21}$ photons/m²/s). Cell movement dynamics in response to directional light stimulation were continuously monitored and recorded using an ATLI scientific-grade microscopy imaging system at a capture rate of 1 frame per minute. All experiments were conducted under controlled temperature conditions (23 \pm 1°C).

3.3 Microscopic observations of cells

For microscopic observations, rectangular glass microcapillaries (0.10 × 2.00 mm, VitroTubesTM model 5012) were employed as optically transparent sample chambers. High temporal-resolution imaging was performed using a Phantom V2512 ultra-highspeed camera (Vision Research) coupled with a Leica DMi8 inverted microscope system, equipped with an advanced zero-drift autofocus unit to ensure sustained focusing stability during prolonged recordings. Prior to experiments, C. reinhardtii cultures were harvested at mid-logarithmic growth phase (OD₆₈₀≈1) to ensure optimal cellular vitality and motility. The algal suspension was diluted to OD₆₈₀=0.5 using TAP medium, and 100 uL of the diluted suspension was loaded into a 0.1 mm × 2 mm rectangular glass microcapillary (the 0.1 mm thickness constrained algal movement range to facilitate subsequent data processing). The microcapillaries were mounted on microscope slides and positioned under the Leica DMi8 microscope. For quantitative analysis of dynamic cellular motility patterns, bright-field image sequences were acquired at 1000 frames per second (fps) using a 40×/0.60 NA objective. To ensure statistical robustness, a minimum of three independent biological replicates (n≥3) were performed for each experimental condition, with each replicate dataset comprising 10,000-15,000 consecutive frames (equivalent to 10-15 seconds of continuous recording at 1000 fps).

3.4 Micromanipulation of cells

We performed micromanipulation experiments using custom-made glass-bottom dishes (2 mm thickness) for microscopic observations. Image acquisition was conducted using a Teledyne Photometrics camera mounted on a Nikon Eclipse Ti2-E microscope. The HMS-320D-S micromanipulation system (Huayue Medical, China) equipped with 2.5 μm micropipettes was employed to immobilize individual cells in liquid medium for subsequent observation. Bright-field images were recorded at 250 frames per second using a 100× oil objective for about 30 seconds. For each algal strain, approximately 10 individual cells were sampled for data compilation.

3.5 Image analysis

Image analysis was performed in a similar way as described in reference¹⁸. Based on microbial microscopic tracking algorithms, our image analysis enabled the acquisition of morphological and positional information of microbial cells at each time point. Then, the cell speed can be calculated as $v = |r(t+\tau)-r(t)|/\tau$, with r(t) representing the position vector of the examined cell at time t, τ denoting the time lag. The cell trajectory was reconstructed by connecting the central coordinates of cellular positions in each image frame; Mean squared displacement (MSD) analysis was performed according to reference¹⁹, where $MSD(\tau) = \langle |r(t+\tau)-r(t)|^2 \rangle$, and $\langle \rangle$ indicates ensemble averaging. Using ImageJ, the displacement positions of cells during the observation period can be overlaid onto a single image to generate a cell body superposition plot that visualizes cellular movement over time.

For the cilium image analysis, the skeleton of each cilium was first generated, and its start point (basal body point) and end point were determined. Then, three parameters θ , α and β were defined (see the definitions in the text) and used to characterize the beating behavior of the cilium. To judge the two cilia of a cell to beat synchronously is first to calculate the phase shift between the oscillations of α and β for one period, and then the two cilia are said to have synchronized beating if the phase shift is no larger than 0.004s (1 frame).

4. Results

4.1 C. reinhardtii cells lost phototactic behavior in the absence of TLP2

A *C. reinhardtii* cell possesses a red eyespot at its anterior end, which detects light intensity and direction, enabling phototactic behavior through cilia motility²⁰. The phototactic response in *C. reinhardtii* represents a photoreceptor-mediated proactive defense strategy, which can help to mitigate photodamage and maintain energy homeostasis under photoinhibitory conditions²¹.

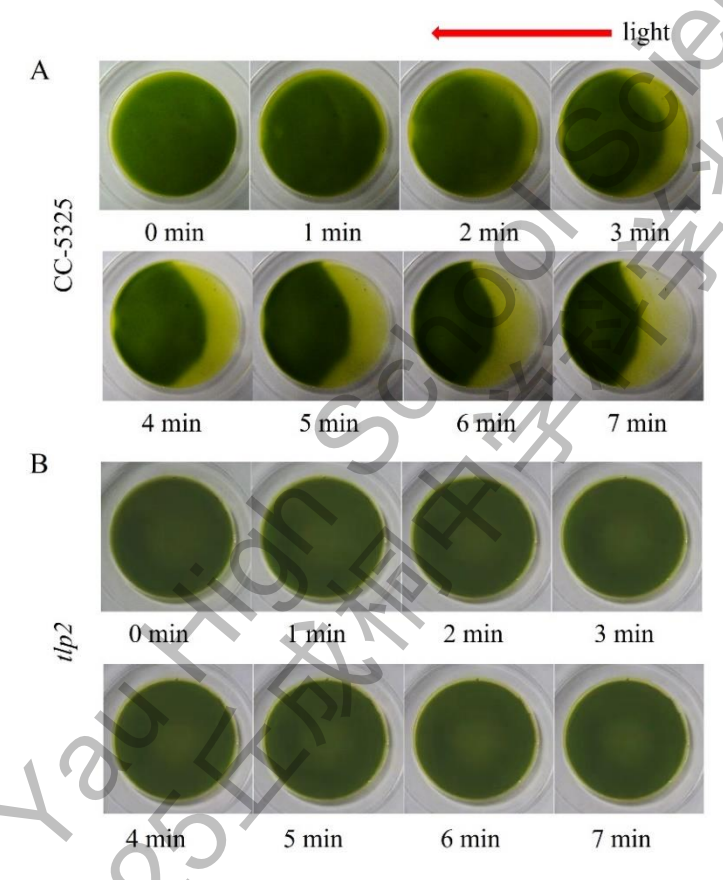


Figure 2. Phototactic response assay of CC-5325 and *tlp2*. A. Phototactic behavior of CC-5325 under flashlight illumination during the first 7 minutes. B. Response of *tlp2* mutant under the identical illumination conditions during the first 7 minutes. The light source was placed at the right side of the dish.

To investigate the impact of *tlp2* deletion on phototactic behavior, we employed the classical dish assay (Figure 2). When exposed to directional flashlight illumination, CC-5325 exhibited a trend of moving away from the light source (i.e. negative phototaxis) within 2 minutes. By 4 minutes, a distinct crescent-shaped distribution pattern formed. At 7 minutes, the right side of the dish (i.e., the side closer to the light

source) was nearly devoid of green coloration, indicating that the majority of cells migrated away from the light source. In contrast, the *tlp2* mutant showed no response in 7 minutes under the identical illumination condition.

4.2 tlp2 showed different characteristic swimming motility than WT cells

The phototactic behavior of *C. reinhardtii* cells is driven by cellular swimming motility powered by ciliary beating. To further understand the role of TLP2 in regulating cell motility, next we characterized the motility behavior of cells at the single cell level for both CC-5325 and *tlp2* mutant.

Using microscopic tracking techniques, we first obtained the trajectories of cells. Figure 3 shows a part of cell trajectories that this study obtained for CC-5325 and *tlp2*. In terms of trajectory shape, CC-5325 cells exhibited predominantly smooth and linear or curvilinear trajectories (Figure 3A), whereas *tlp2* cells showed more tortuous paths with increased frequency of wavy and helical/spring-like movement patterns (Figure 3B). Throughout the 60-second microscopic recording period (Supplementary Movies S1 and S2), we found that all observed CC-5325 cells remained motile. Interestingly, for *tlp2* cells, approximately 65% of cells are freely motile, while the remaining 35% adhered to the glass surface and remained immotile (Figure 4A), with their cilia straightened and firmly attached (Figure 4B).

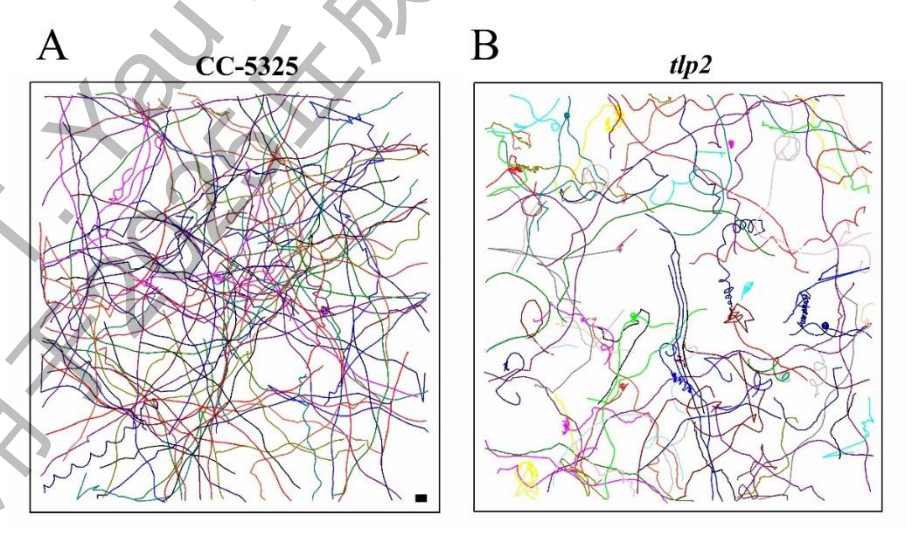


Figure 3. Examples of cell trajectories of CC-5325 and *tlp2* obtained in this study for an observation time window of 60s. A. Movement trajectories of CC-5325. B. Movement trajectories of *tlp2*. Different colors in the figure represent distinct individual cells. Cell images were recorded under a 40x objective. Scale bar: 20 μm.

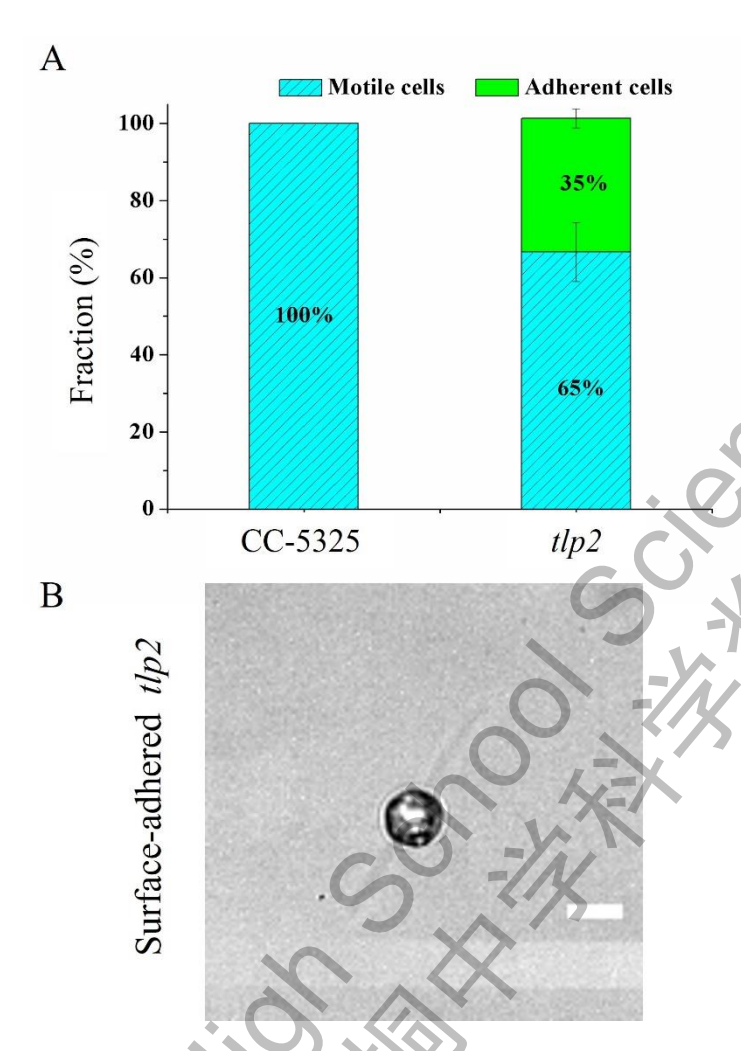


Figure 4. Proportion of motile and adherent cells. A. Proportion of motile and adherent cells for CC-5325 and *tlp2* within a 60s observation period. B. An example showing a *tlp2* cell adhered to a glass surface. Scale bar: 20 μm.

Quantitatively, we calculated the swimming speed of motile cells in both CC-5325 and tlp2. The results revealed distinct speed distribution profiles between the two strains (Figure 5). CC-5325 cells demonstrated a range of swimming speed from 50 to 175 μ m/s, with a prominent peak at 125 μ m/s, while the speed distribution of tlp2 cells is left-shifted with a reduced speed range (50~150 μ m/s) as well as a smaller peak speed at 75 μ m/s (Figure 5A). Consequently, CC-5325 has a higher average swimming speed of 120 \pm 28 μ m/s than that of tlp2, which is 92 \pm 41 μ m/s (Figure 5B). These results suggest that the swimming motility in tlp2 cells was impaired.

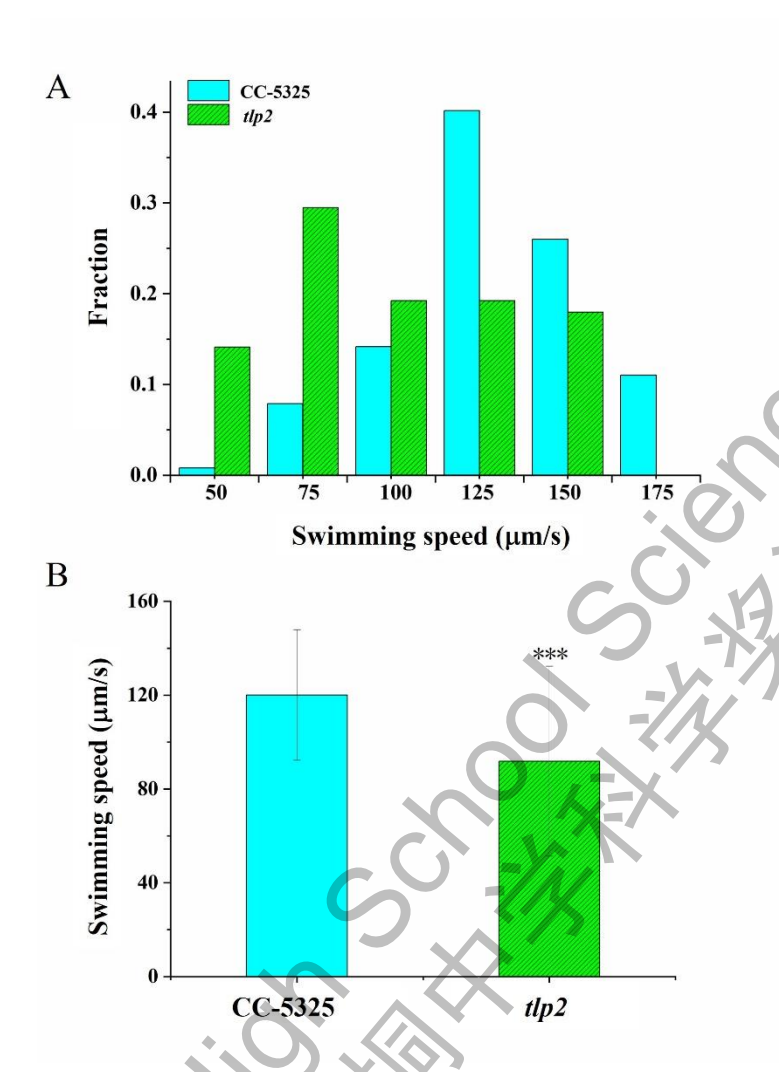


Figure 5. Swimming speed of CC-5325 and tlp2 cells. A. Instantaneous speed distribution of two strains. B. The average swimming speed of two strains. Statistical significance was measured using a two-sample Student's t-test. ***p very highly significant at p < 0.001.

The motion of cells in liquid can include both active process (through swimming) and passive process (through diffusion). A common way to evaluate the different effects of active process and passive process is to calculate the mean squared displacement (MSD), which is a parameter used to measure the deviation of a type of motion from a random diffusive motion. In the log-log plot of $MSD(\tau)$ versus τ , the slope of the curve reflects the nature of the type of motion: a slope of 1 indicates a Brownian-type motion, while >1 is super-diffusive and <1 is sub-diffusive. In this study, to further understand the differences of two strains in swimming motility, we also applied the MSD analysis to quantify the trajectories of two strains. Both CC-5325 and tlp2 exhibited a MSD

curve with a slope greater than 1 in the log-log plot (Figure 6), indicating that cells of both strains performed super-diffusive motion, which are expected as cells can swim actively. However, *tlp2* displayed a relatively lower MSD slope compared to CC-5325, indicating a less active motion, which is consistent with the observed decrease in the average swimming speed in *tlp2*. Together, these results support that TLP2 play important roles in facilitating normal swimming motility of cells.

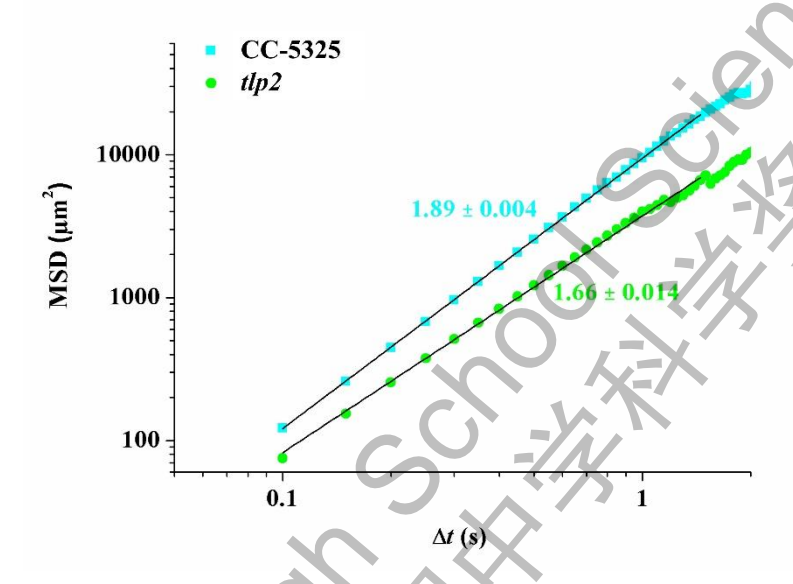


Figure 6. Mean squared displacements (MSDs) of CC-5325 and *tlp2***.** The lines are fitted results in the log-log plot.

4.3 The swimming motility differences between two strains arise from different beating behavior of cilia

C. reinhardtii modulates its motility through precise regulation of the beating patterns and waveforms of its two cilia^{22,23}. Generally, ciliary beating can be classified into two types of modalities, symmetrical beating and asymmetrical beating. The symmetrical beating is characterized by the synchronous, in-phase oscillation of both cilia (see one example in Figure 7, also shown in Supplementary Movie S3). They propel backward from the anterior end in a breaststroke-like pattern, generating maximum forward thrust. This mode is the principal mechanism to power forward locomotion, enabling the cell to swim in a steady linear or curvilinear trajectory at speeds ranging approximately from 100 to 200 μm/s.

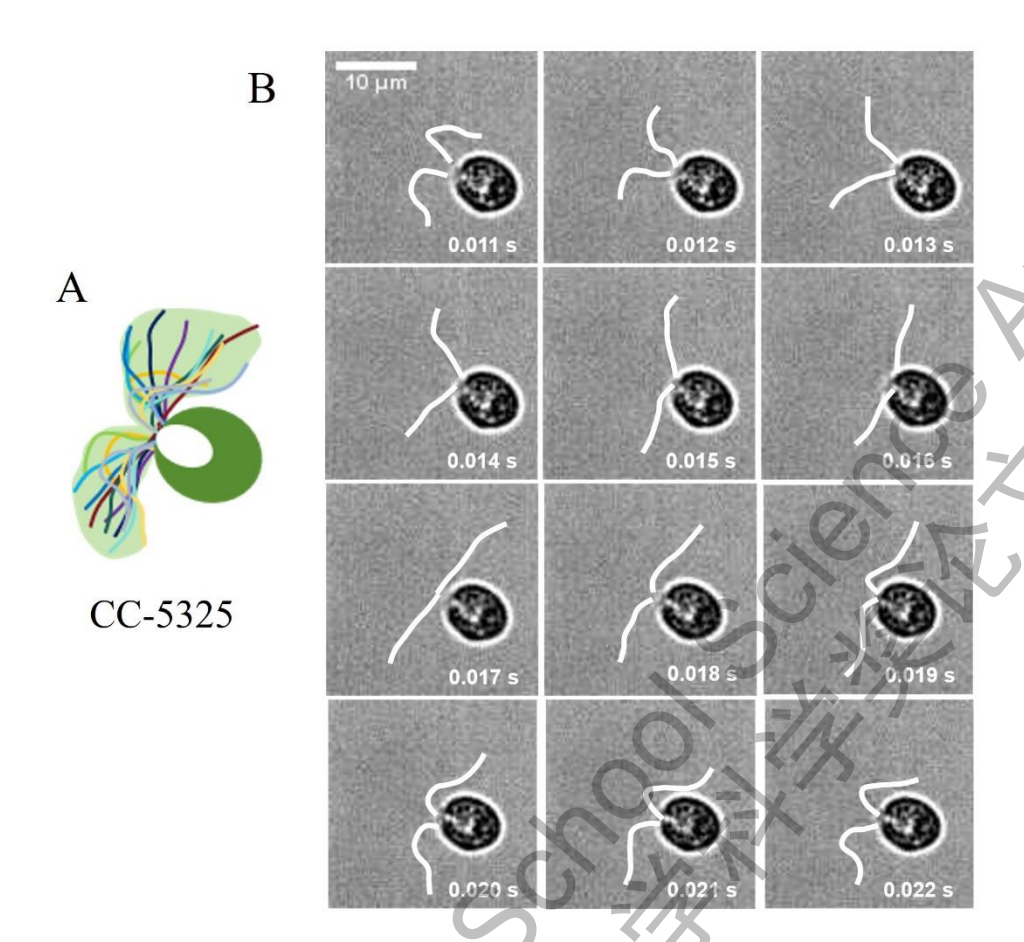


Figure 7. An example illustrates a complete cycle of ciliary symmetric beating of a CC-5325 cell. A. Overlay of a complete ciliary beating cycle. Different colors represent successive ciliary positions at different time points. The light green shaded area indicates the region swept by the cilium over one cycle. B. A time series of snapshots in one cycle of ciliary symmetric beating. In each snapshot, the cilia were marked with white segments manually. Scale bar: 10 μm.

In contrast, the asymmetrical beating pattern arises from a dyssynchrony in ciliary activity, where one cilium alters its beating, typically demonstrating a reduced efficiency or an aberrant, asymmetric waveform, while the contralateral cilium continues its effective power strokes (see one example in Figure 8, also shown in Supplementary Movie S4). This imbalance in propulsive forces results in distinctive cellular behaviors such as phototactic turning, erratic rotation around a fixed point, or even backward movement.

Such two types of ciliary beating were both observed in this study, but the occurrence frequencies are different for CC-5325 and *tlp2*. In CC-5325 cells, the symmetrical beating was the dominant one observed, while in *tlp2* the asymmetrical

beating was frequently observed. Because of the different beating modalities, the corresponding cell trajectories generated therefrom also displayed different characteristics (Figure 9), which were also shown in Figure 3.

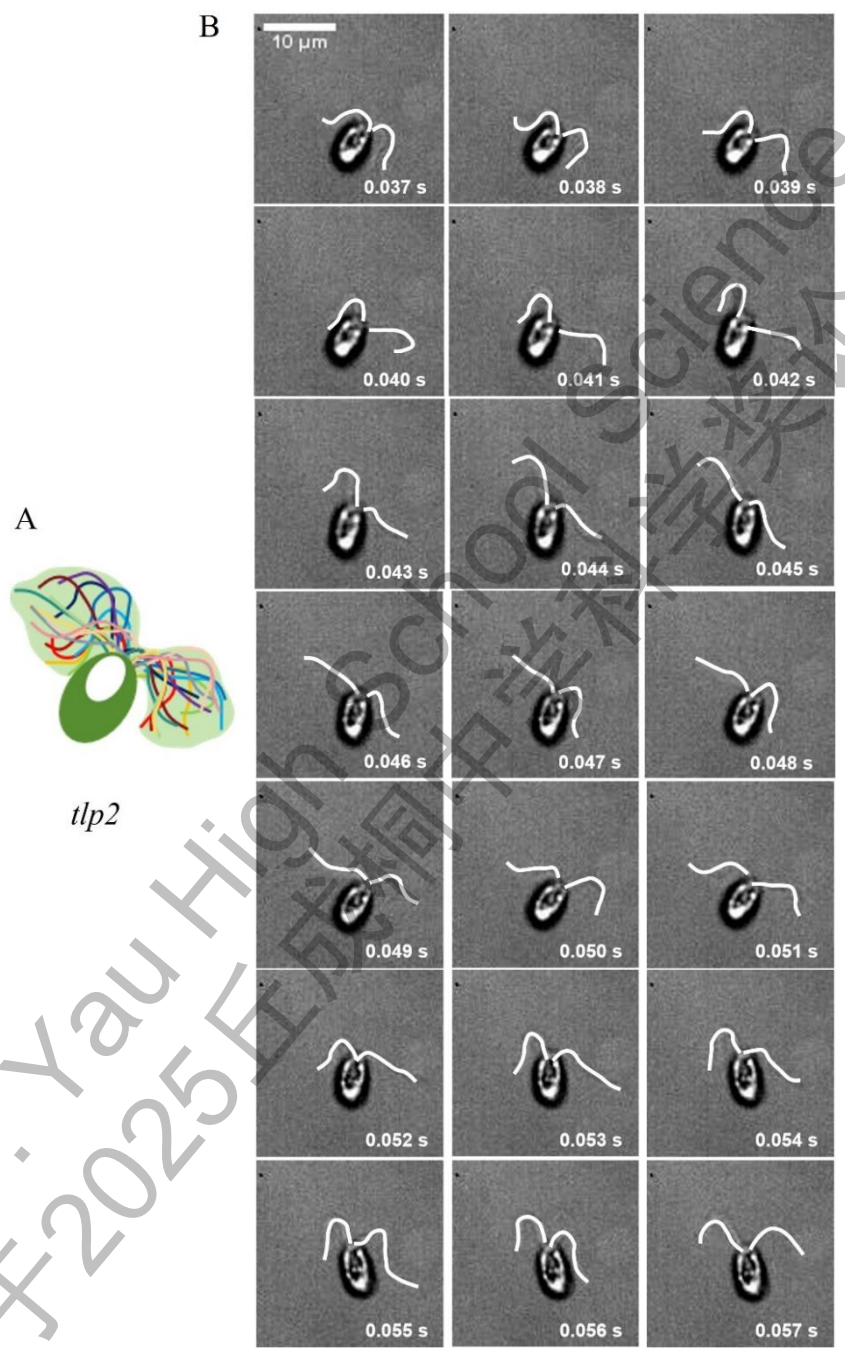


Figure 8. An example illustrates a complete cycle of ciliary asymmetric beating of a *tlp2* cell. A. Overlay of a complete ciliary beating cycle. Different colors represent successive ciliary positions at different time points. The light green shaded area indicates the region swept by the cilium over one cycle. B. A time series of snapshots in one cycle of ciliary asymmetric beating. In each snapshot, the cilia were marked with white segments manually. Scale bar: 10 μm.

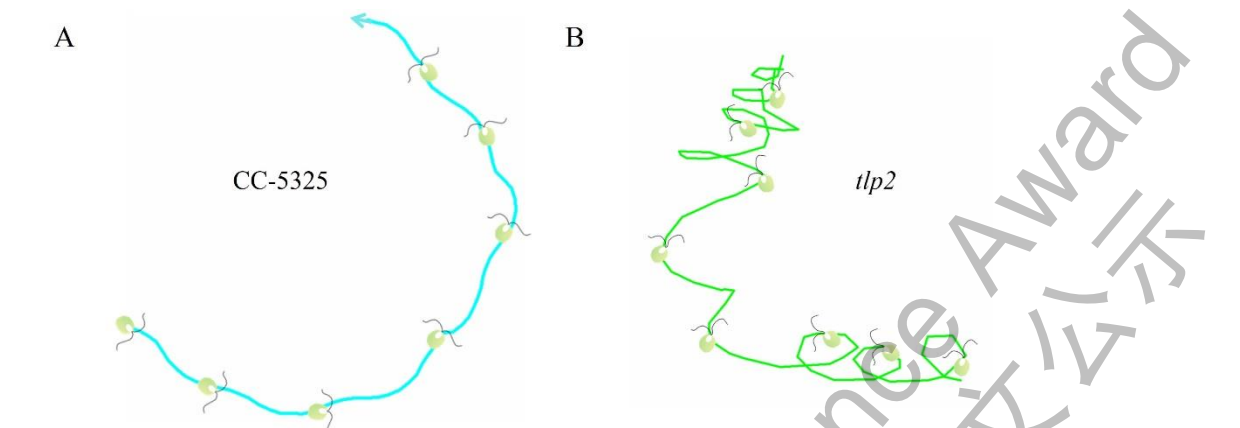


Figure 9. An exemplar cell trajectory overlaid with cell cartoons to schematically illustrate the two ciliary beating modalities and the cell trajectories generated therefrom. A. Symmetric beating of a CC-5325 cell. B. Asymmetric beating of a tlp2 cell. The time interval between successive cell positions is 0.5 s.

To quantitatively characterize the beating pattern of cilia, cilium identification is necessary. We first manually marked the cilia of cells in each image, which enabled us to unambiguously demonstrate the two distinct ciliary beating modalities. Figure 7 illustrates a complete cycle of ciliary symmetrical beating of a CC-5325 cell. Figure 7A shows the area swept by the cilia during their beating, while Figure 7B shows a time series of snapshots of cilia during the beating cycle. In each snapshot, the cilia were marked with white segments manually. Similarly, Figure 8 displays a complete cycle of ciliary asymmetrical beating of a *tlp2* cell.

After tracking the cilia of a cell for one complete beating cycle, then we can tell the synchronization of two cilia. For the two cilia of a C. reinhardtii cell, the one closest to the eyespot is called the cis-cilium/cis-flagellum, and the other is called the trans-cilium/trans-flagellum. In this study, however, since the eyespot could not be reliably identified in our tracking assays, we could not determine confidently which cilium is cis-cilium and which is the other. But this differentiation does not affect our analysis. For the purpose of better presenting our analysis results, here we simply named the two cilia as cilium a and cilium b (Figure 10A). To characterize the synchronization, three angular parameters θ , α and β were employed. As shown in Figure 10A, θ is defined as the angle between the long axis of the cell body and the horizontal direction. It is used to check the status of the cell. α is defined as the angle between the long axis of the

cell body and the line connecting the starting point of the cilium a from the basal body and a chosen point along the filament of cilium a (here, a point that is 30 pixels away from the starting point along the cilium filament was chosen, which is indicated by an orange dot in Figure 10A). β is defined similarly for the cilium b. α and β are used to denote the phase angle of the cilium beating.

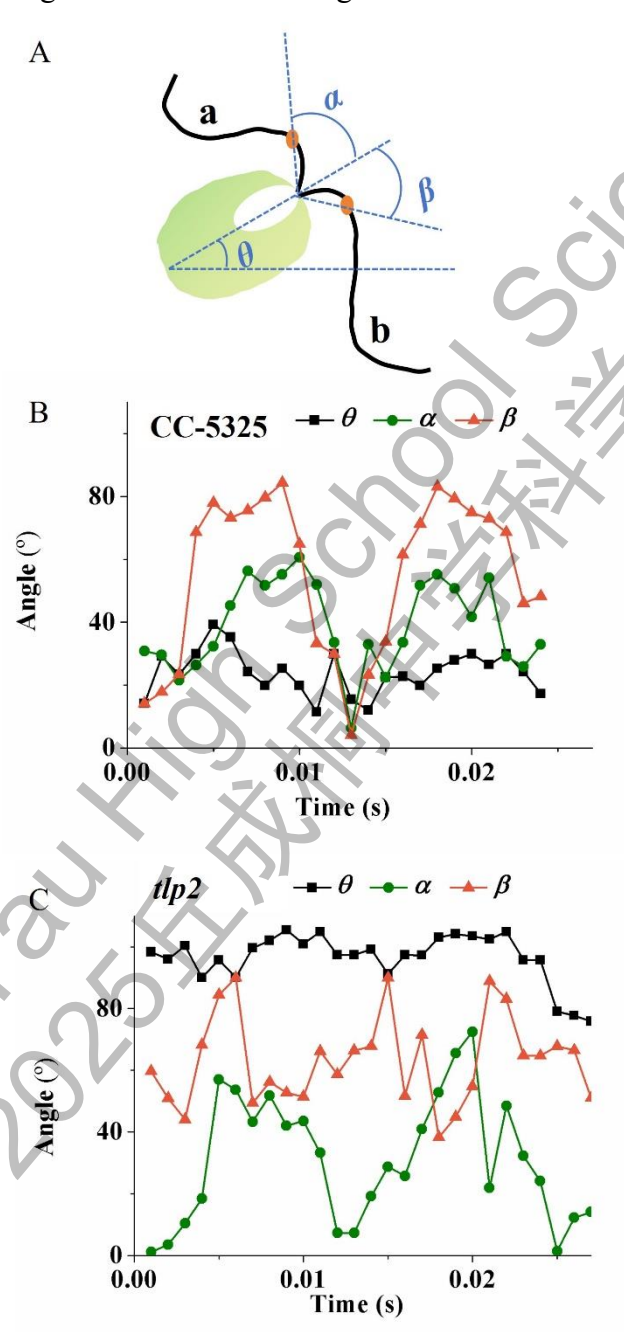


Figure 10. Quantitative analysis on the ciliary beating behavior. A. Schematic diagram showing the two cilia definitions and the three angular parameters θ , α and β . B-C. The change of angular parameters with time over a period of 0.027s (B) for the CC-5325 cell shown in Figure 7, and (C) for the tlp2 cell shown in Figure 8.

Using these parameters, the beating behavior of cilia for the exampled cells shown in Figures 7 and 8 were analyzed, and the results are shown in Figure 10B and 10C. Since for both examples, cells freely swam, θ would fluctuate as expected. Also, due to ciliary beating, α and β for the both CC-5325 and tlp2 cells oscillated. However, in the CC-5325 cell, the oscillations of α and β were in phase and essentially reached maximal and minimal values simultaneously, i.e., the two cilia were synchronized in beating, whereas in the tlp2 cell, the oscillations of α and β were clearly not in phase and the two cilia showed a distinct asynchronous beating pattern. But given the inherit heterogeneity of cells in nature, to get a statistical meaningful conclusion regarding the beating behavior of two strains, more cells need to be analyzed.

Marking cilia manually is tedious and less efficient. Considering the large number of images obtained from microscopy, to mark all the images manually becomes an impossible mission. Therefore, new methods that can identify cilia in each image automatically and accurately are in urgent need. Artificial intelligence (AI) techniques recently have shown great potential in image processing²⁴. So, in this study, we tried to develop an AI-assisted method to deal with the identification of cilia and analysis their beating patterns in a more efficient and high-throughput way.

Professor Fan's lab has already developed an AI-assisted model based on an open-source tool-Cellpose²⁴ for microbial image processing. Based on this model, we need to tune the parameters by training the model with manually labelled images as the training dataset.

Unfortunately, after 400 rounds of model training, the performance of the model was still not satisfactory (Figure 11), which is due to inherent limitations in the set-up of microscope imaging for freely swimming cells—specifically, the difficulty in maintaining both cilia within the same focal plane during the freely swimming of a cell. Such technical difficulties precluded robust tracking of a complete ciliary beat cycle for freely swimming cells.

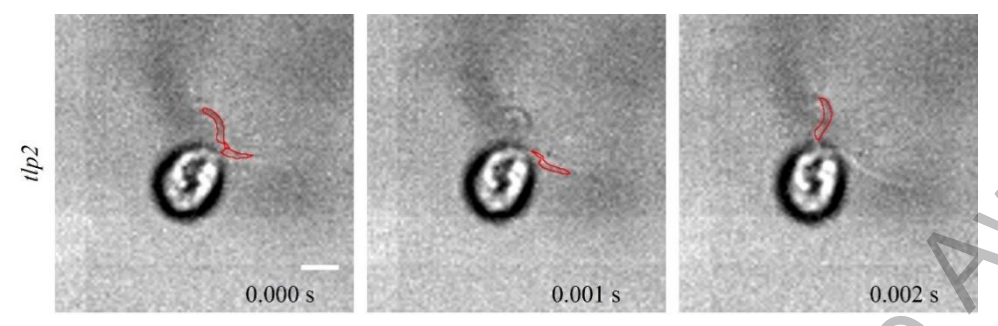


Figure 11. Examples showing the poor identification results (marked in red) through AI-assisted model for freely swimming cells. Scale bar: 10 µm.

4.4 Statistical analysis of immobilized cells through micromanipulation revealed the impaired synchronization of ciliary beating in *tlp2* cells

To overcome the technical challenges in ciliary identification of freely swimming cells, we employed micromanipulation techniques to immobilize individual *C. reinhardtii* cell by holding it with a 2.5 µm diameter micropipette under the microscope. Figure 12 shows the equipment set-up.

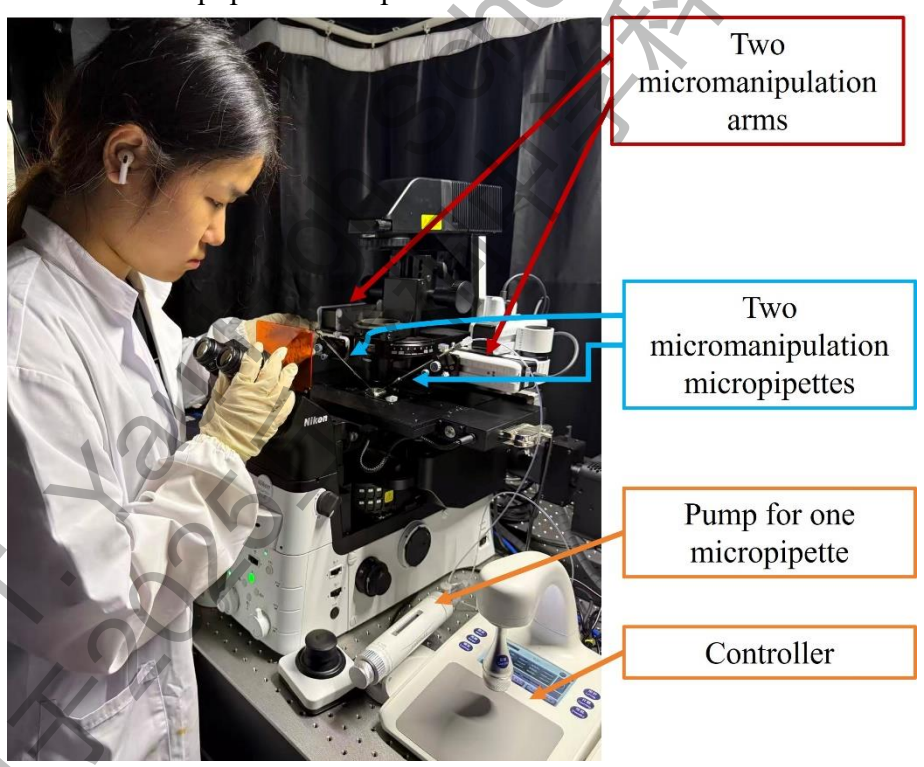


Figure 12. Micromanipulation equipment set-up. The photo was captured during the adjustment of micropipettes.

This immobilization strategy enabled prolonged tracking of ciliary beating in a single cell and significantly increased the probability of both cilia remaining within the same focal plane. After training the AI-assisted model with the data obtained using

micromanipulation techniques, the performance of the model was much more improved. Figure 13 shows examples of ciliary identification results obtained from the AI-assisted model. In each image, a *C. reinhardtii* cell was held by a micropipette, and the outline of the identified cilia through the model were marked in red and overlaid with the original image. The results demonstrate a good agreement between model-identified cilia and true cilia (judged by human eyes).

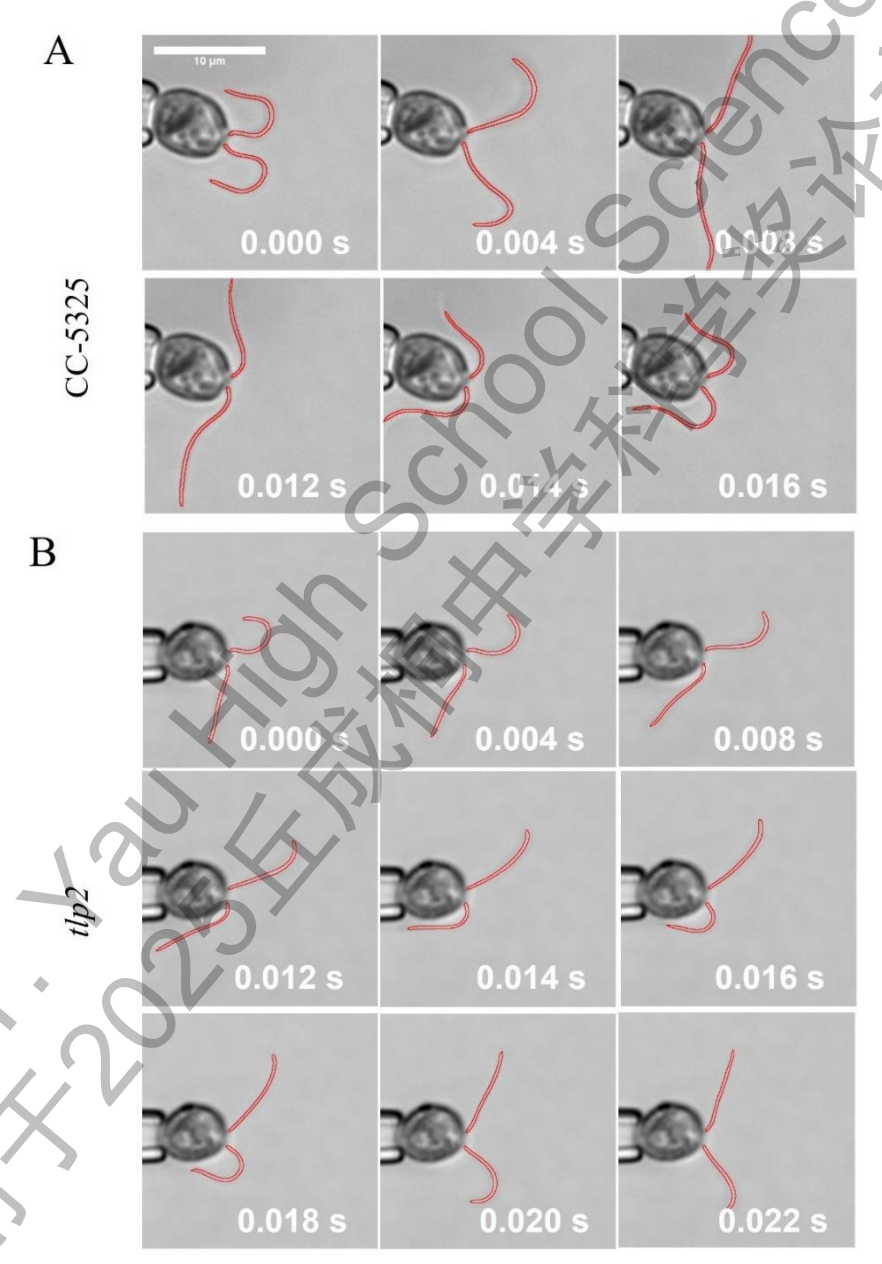


Figure 13. Examples of cilia identification of a cell through AI-assisted model. The cell was held by a micropipette, and these snapshots showing the identified cilia whose outlines were marked in red and overlaid with each original image at different time points. A. a CC-5325 cell. B. a *tlp2* cell. Scale bar: 10 μm.

Using this AI-assisted model, we did a quantitative analysis on the dynamics of ciliary beating behavior for both CC-5325 and tlp2 cells. We first measured the beating periodicity for each cilium of a cell. The results are shown in Figure 14. For a CC-5325 cell, cilium a and cilium b have very similar distributions of beating periods, and the averaged beating period is 0.022 ± 0.004 s for cilium a, and 0.025 ± 0.004 s for cilium b, which are essentially identical considering the variance of measurements. In contrast, for a tlp2 cell, cilium a and cilium b have significantly different beating period distributions with an averaged beating period 0.029 ± 0.012 s for cilium a, while 0.038 ± 0.016 s for cilium b.

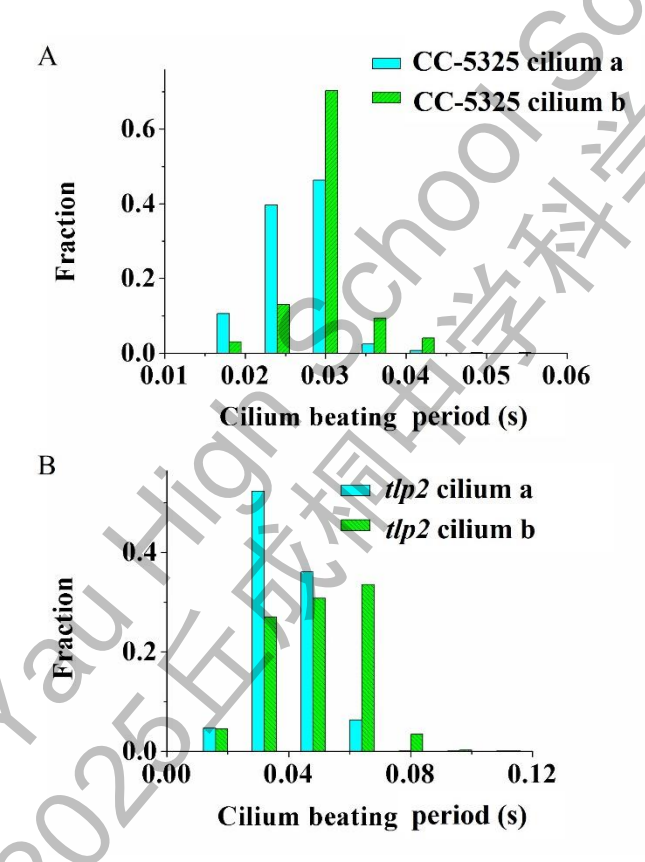


Figure 14. Distributions of measured beating periods for the two cilia (cilium a and cilium b) of a cell. A. Distributions of measured beating periods in CC-5325 cells. B. Distributions of measured beating periods in *tlp2* cells. For all cases, the number of analyzed beating period is more than 1500.

Similar to the case of freely swimming cells, for the cells held steadily by micropipettes, we also investigated the synchronization status of the two cilia, again using the parameters θ , α and β . The time evolution of the three parameters over a 0.10s period are shown in Figure 15. Compared with the freely swimming cells shown in

Figure 10, the behavior of θ is clearly different, as θ in Figure 15 essentially didn't oscillate and stayed at the same level for both CC-5325 and tlp2, which is expected for these immobilized cells. But such immobilization through micropipette didn't affect the ciliary beating, as both α and β displayed oscillating behavior, similar to Figure 10. Moreover, because this immobilization method enabled prolonged tracking of ciliary beating, whether the two cilia beat in a synchronized way or not is easier to tell. In Figure 15A, α and β curves are essentially overlapped with each other, indicating the identical phase and amplitude of the beating between two cilia of the CC-5325 cell, so the two cilia were synchronized. By contrast, in Figure 15B, α and β do not have a stable phase shift although their amplitudes are similar, indicating that the two cilia of the tlp2 cell were not synchronized.

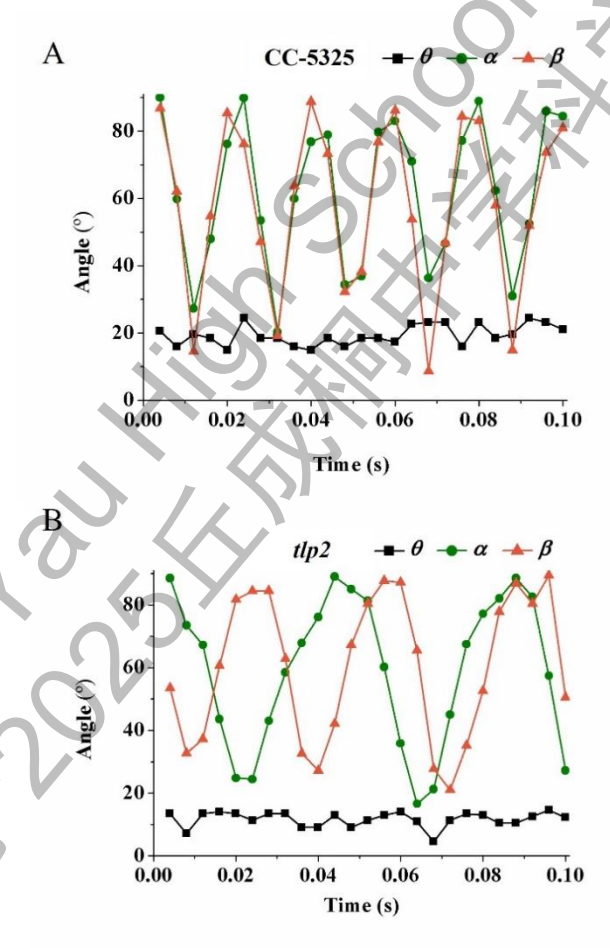


Figure 15. Quantitative analysis on the ciliary beating behavior for cells held by a micropipette. A. The change of angular parameters with time over a period of 0.1s for a CC-5325 cell. B. The change of angular parameters with time over a period of 0.1s for a *tlp2* cell.

Synchronized ciliary beating is beneficial for a cell to have a powerful thrust to move quickly, but this may not be needed always, and under some circumstances such as when cells turn their moving directions, asynchronized ciliary beating would appear. Thus, to further understand the synchronization behavior of ciliary beating, we also measured the proportion of time during which the two cilia of a cell exhibited a synchronized beating over a one-minute observation window (Figure 16). The results clearly show that CC-5325 cells maintained a symmetrical beating pattern for $58.9 \pm 0.6\%$ of the duration of observation, whereas tlp2 cells were observed to display such coordinated pattern for only about $17.8 \pm 0.2\%$ of the observation time. These pronounced discrepancies in ciliary beating coordination is likely a major contributor to the observed differences in swimming motilities and hence phototactic behaviors of the two strains.

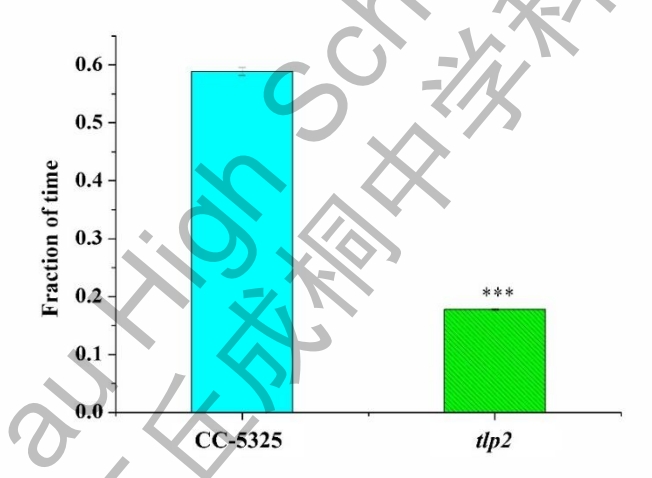


Figure 16. Fraction of time with synchronized ciliary beating within a one-minute period for both CC-5325 and tlp2 cells. Statistical significance was measured using a two-sample Student's t-test. ***p very highly significant at p < 0.001.

5. Discussions

This study systematically investigated the critical role of TLP2 protein in regulating motility in *C. reinhardtii* at three different scales, including macroscopic (populational), cellular, and ciliary scales.

Firstly, at the macroscopic level, the TLP2 mutant completely lost phototaxis

(Figure 2). This result indicates that the absence of TLP2 disrupts the cell's ability to appropriately response to environmental light signals. Phototaxis is a core survival strategy for *C. reinhardtii* to find optimal light conditions for photosynthesis. The loss of this behavior implies severely impaired adaptability and competitiveness in the natural environment for the mutant.

At the cellular scale, our results revealed multiple abnormal motility behavior caused by the TLP2 deletion: approximately 35% of cells became completely inactive and adhered to the substrate (Figure 4), while the swimming speed of the remaining motile cells was significantly reduced (Figure 5). Their movement trajectories changed from the smooth linear/curvilinear paths of the wild type to the more tortuous, wavy paths of TLP2 mutant (Figure 3). MSD analysis further confirmed their reduced effective motility (Figure 6). These phenotypes, together with the results at the macroscopic level, are highly consistent with recent findings in mice¹³, where *tulp2* knockout mice exhibit oligoasthenoteratozoospermia, which is frequently reported in male infertility cases²⁵ and characterized by decreased sperm count, reduced motility, and tail deformities¹³. Our study directly corroborates, in *C. reinhardtii*, the evolutionarily conserved function of TULP2/TLP2 in driving cell motility. Increased cell adhesion of TLP2 mutant might stem from altered surface properties due to changes in ciliary membrane protein compositions, while changes in speed and trajectory directly point to dysfunction of the propulsion apparatus—the cilia themselves.

A more interesting discovery came from the fine analysis of the ciliary beating patterns, which was much improved by micromanipulation techniques. The two cilia of wild-type cells (CC-5325) had similar beat periods (~0.022-0.025 s) and maintained synchronous, symmetric beating (the "breaststroke" pattern) for nearly 60% of the time, which is the basis for efficient linear propulsion (Figure 13A, Figure 14A). In contrast, the beat periods of the two cilia in *tlp2* were not only significantly longer but also vastly different from each other (0.029 s vs. 0.038 s), causing the time of symmetric beating to plummet to less than 18% (Figure 13B, Figure 14B). This severe dyssynchrony explains all the abnormal motility behavior observed at the cellular scale: asymmetric

beating generates a net torque, causing the cell to spin in place or move along a tortuous path rather than swimming straight; the reduced beat frequency and efficiency directly lead to decreased swimming speed.

In this study, we haven't investigated the mechanisms at the molecular level behind the observed abnormal ciliary beating patterns. One intriguing possible mechanism might lie in the regulation of ciliary beating function by TLP2 via altering the cilia structures. Another possible mechanism might rely on the role of TLP2 in regulating the trafficking of cilium, which aligns with the role of the TLP protein family as IFT adapters¹². Its absence can prevent key receptors for light perception and/or transduction (such as photoreceptor proteins in the eyespot) from being properly anchored in the ciliary membrane or disrupts the signaling pathway¹², thereby breaking the entire chain from signal reception to behavioral output. But more studies are needed in the future to test these possibilities.

6. Conclusion

This study employed an integrated approach combining population behavioral assays, single-cell motility analysis, and high-speed imaging to comprehensively elucidate, for the first time and at multiple scales, the regulatory role of TLP2 protein in *C. reinhardtii* motility. The main conclusions are as follows:

TLP2 is essential for phototactic behavior in *C. reinhardtii*. Its absence completely abolished the cells' photoresponse capability at the population scale; TLP2 deficiency caused severe cell motility dysfunction, manifested as inactivation of a subset of cells to be non-motile, a significant reduction in swimming speed of motile cells, and a transition of movement trajectories from linear to tortuous paths; The core function of TLP2 lies in maintaining the synchronization of cilia beating. Its loss led to heterogenous and prolonged beat periods of the two cilia and severely disrupted the maintenance of the symmetric beating pattern. This is the direct cause of all observed motility phenotypes.

Using cell movement and ciliary beating as directly observable and quantifiable outputs, this study demonstrated a good practical way to evaluate the functions of TLP2,

which extends the routine molecular or macroscopic approaches. The findings in this study will further deepen our understandings of TLP2 in the regulation of cilia-driven motility and thus provide insight for developing new strategies in combating flagella/cilia-related diseases. Particularly, given the similarity in the motility phenotypes of TLP2 mutant and the sperm cells of oligoasthenoteratozoospermia, the findings of this study may be especially beneficial for the clinical applications of the diagnosis and treatment of oligoasthenoteratozoospermia. In addition, the developed high-throughput AI-assisted image processing method provides a useful tool for data processing of microscopic images and can be readily extended to other related scenarios.

7. References

- Pala, R., Jamal, M., Alshammari, Q. & Nauli, S. M. The roles of primary cilia in cardiovascular diseases. *Cells* **7**, 233 (2018).
- Gilpin, W., Bull, M. S. & Prakash, M. The multiscale physics of cilia and flagella. *Nat Rev Phys* **2**, 74-88 (2020).
- Goldstein, R. E. Green algae as model organisms for biological fluid dynamics. *Annu Rev Fluid Mech* **47**, 343 (2014).
- Witman, G. B. Chlamydomonas phototaxis. *Trends Cell Biol* 3, 403 (1993).
- Reiter, J. F. & Leroux, M. R. Genes and molecular pathways underpinning ciliopathies. *Nat Rev Mol Cell Biol* **18**, 533-547 (2017).
- Papon, J. F. et al. Quantitative analysis of ciliary beating in primary ciliary dyskinesia: a pilot study. *Orphanet J Rare Dis* 7, 1-11 (2012).
- Weng, Z., Xu, W., Zheng, Y. Biological functions of the TULP family members and pathogenetic mechanism of their associated diseases. *Chin Bull Life Sci* **35**, 11 (2023).
- 8 Coleman, D. L. & Eicher, E. M. Fat (fat) and Tubby (tub): Two autosomal recessive mutations causing obesity syndromes in the mouse. *J Hered* **81**, 424-7 (1990).
- Noben-Trauth, K., Naggert, J. K., North, M. A. & Nishina, P. M. A candidate gene for the mouse mutation tubby. *Nature* **380**, 534-538 (1996).
- Ullah, I., Kabir, F., Iqbal, M., Gottsch, C. B. S. & Riazuddin, S. A. Pathogenic mutations in TULP1 responsible for retinitis pigmentosa identified in consanguineous familial cases. *Mol Vis* 22, 797-815 (2016).
- Norman, R. A. et al. Tubby-like Protein 3 (Tulp3) regulates patterning in the mouse embryo through inhibition of sonic hedgehog signaling. *Hum Mol Genet* **18**, 1740-54 (2010).
- Han, S. *et al.* TULP3 is required for localization of membrane-associated proteins ARL13B and INPP5E to primary cilia. *Biochem Biophys Res Commun* **509**, 227-234 (2019).
- Zheng, M., Chen, X., Cui, Y., Li, W. & Zhu, H. TULP2, a new RNA-binding protein, is required for mouse spermatid differentiation and male fertility. *Front Cell Dev Biol* **9**, 623738 (2021).
- Legal, T. *et al.* Structure of the ciliary tip central pair reveals the unique role of the microtubule-seam binding protein SPEF1. *Curr Biol* **35**, 3404-3417 (2025).
- Liu, Y., Li, W., Zhang, R., Sun, S., and Fan, Z. Unraveling the intricate cargo-BBSome coupling mechanism at the ciliary tip. *Proc Natl Acad Sci* **120**, e2218819120 (2023).
- Xue, B. et al. Intraflagellar transport protein RABL5/IFT22 recruits the BBSome to the basal body through the GTPase ARL6/BBS3. *Proc Natl Acad Sci* **117**, 2496-2505 (2020).
- Liu, Y., Xue, B., Sun, W., Wingfield, J., Sun, J., Wu, M., Lechtreck, K. F., Wu, Z., Fan, Z. Bardet–Biedl syndrome 3 protein promotes ciliary exit of the signaling protein phospholipase D via the BBSome. *eLife*, **10**:e59119 (2021).

- Zhang, J. *et al.* Oscillation of type IV pili regulated by the circadian clock in cyanobacterium Synechococcus elongatus PCC7942. *Sci Adv* **10**, 12 (2024).
- Oakes, P. W., Patel, D. C., Morin, N. A., Zitterbart, D. P. & Tang, J. X. Neutrophil morphology and migration are affected by substrate elasticity. *Blood* **114**, 1387-1395 (2009).
- 20 Sineshchekov, O. A., Jung, K. H. & Spudich, J. L. Two rhodopsins mediate phototaxis to low- and high-intensity light in Chlamydomonas reinhardtii. *Proc Natl Acad Sci* **99**, 8689-8694 (2002).
- Berthold, P. *et al.* Channelrhodopsin-1 initiates phototaxis and photophobic responses in Chlamydomonas by immediate light-induced depolarization. *Plant Cell* **20**, 1665-1677 (2008).
- Guo, H., Man, Y., Wan, K. Y. & Kanso, E. Intracellular coupling modulates biflagellar synchrony. *J R Soc Interface* **18**, 20200660 (2021).
- Wei, D., Quaranta, G., Aubin-Tam, M. E. & Tam, D. S. W. The younger flagellum sets the beat for Chlamydomonas reinhardtii. *eLife* **13**:e86102 (2024).
- Pachitariu, M., Rariden, M. & Stringer, C. Cellpose-SAM: superhuman generalization for cellular segmentation. *bioRxiv* 2025.04.28.651001 (2025).
- Colpi, G. M., Francavilla, S., Haidl, G., et al., European academy of andrology guideline management of oligo-astheno-teratozoospermia, *Andrology* **6**, 513-524 (2018).

8. Legends of supplementary movies

Movie S1. An example showing the normal swimming motility of CC-5325 cells. In this case, essentially all appeared cells in the field of view were motile. The movie was taken at a frame interval of 0.005s (i.e. 200 fps) for 60s, and was played back with 1 frame out of every 40 frames at a rate of 10 fps. Scale bar, $10 \mu m$.

Movie S2. An example showing the motility behavior of tlp2 cells. In this case, approximately 65% of cells were freely motile, while the remaining 35% adhered to the glass surface and remained immotile. The movie was taken at a frame interval of 0.005s (i.e. 200 fps) for 60s, and was played back with 1 frame out of every 40 frames at a rate of 10 fps. Scale bar, 10 μ m.

Movie S3. An example showing the synchronized, symmetric beating of the two cilia of a CC-5325 cell. The movie was taken at 1000 fps for 0.05s, and was played back at 10 fps. Scale bar, 10 μ m.

Movie S4. An example showing the asymmetric beating of the two cilia of a tlp2 cell. The movie was taken at 1000 fps for 0.1s, and was played back at 10 fps. Scale bar, 10 μ m.

9. Acknowledgement

This research journey began with my deep interests in rare diseases and the underlying mechanisms that cause them. In my school, I started a Children for Children (C4C) organization that aims to support children with rare diseases and raise public awareness. Throughout my preliminary reading on rare disease related papers, I learned that many rare diseases are linked to the defects in cilia, which are hair-like surface appendages of eukaryotic cells. For instance, the Bardet-Biedl syndrome is a rare genetic disease which has typical clinical features including retinal degeneration, learning disabilities, polydactyly, obesity and renal defects. Studies show that it is caused by mutations of genes encoding for cilium-related proteins. In fact, after reading more literature, I learned that there is a wide range of diseases, known as ciliopathies, are closely related to the defects in either the assembly or functions of cilia. Thus, I was fascinated by these tiny yet "magic" nanomachines-cilia.

Meanwhile, I was joining Professor Zhen-Chuan Fan's lab at Zhejiang University for scientific training, where I was introduced to *Chlamydomonas reinhardtii*, a green alga used as a powerful model organism for studying ciliary structures and functions. *C. reinhardtii* is particularly valuable due to its simple unicellular architecture, well-developed genetic tools, and structural conservation of cilia with higher eukaryotes. Professor Fan's lab has constructed a TLP2-null mutant. Through literature, I learned that TLP2 is related to cilia functions, as in mice loss of TLP2 leads to male sterility. However, the mechanisms are still not clear yet.

Then, after discussing with both Professor Fan and my teacher Dr. Han Wang, we decided to start a project on this subject. Specifically, the aim of my project is to understand mechanistically how the motility behavior of *C. reinhardtii* will be affected by TLP2, thus, to reveal the role of TLP2 in the regulation of cilia-driven motility of cells.

Throughout this process, I encountered many challenges. For instance, culturing and maintaining *C. reinhardtii* strains required precise light and nutrient conditions, and early attempts often failed. Not even mention the numerous troubleshooting that I

experienced when operating facilities such as microscopes. With the patient support of many people, I developed the skills to overcome these obstacles and finished the project.

There are many people I would like to thank. Firstly, I would like to express my sincere gratitude to Professor Zhen-Chuan Fan (uncompensated) for his expert guidance throughout the project. I was actively involved in his lab doing the experimental design, data acquisition, and analysis, including microscopic imaging and motility assays. The initial draft of this report was written by me, with valuable feedbacks from both Professor Fan and Dr. Wang. Secondly, I am also thankful to Dr. Han Wang (uncompensated) from my school for his unwavering support and encouragement. I benefited a lot from discussions with him during the whole project. Many thanks to the lab members of Professor Fan's lab for kindly teaching me and helping me whenever I encountered technique problems.

This experience has profoundly enhanced my understanding of molecular biology, genetic engineering, and the pathological basis of rare diseases. It has strengthened my resolve to contribute to the study of ciliopathies and their potential treatments. I am grateful for the opportunity to have taken part in meaningful scientific inquiry and to have received guidance from such dedicated mentors.

From my perspective, this project was not only a scientific exploration but also a personal journey of problem-solving and discovery. It allowed me to connect fundamental cell biology with human health, to appreciate the power of model organisms, and to gain first-hand experience in overcoming experimental challenges. Most importantly, it gave me the confidence to pursue future research with independence and persistence.